# We are IntechOpen,
# the world's leading publisher of
# Open Access books
# Built by scientists, for scientists

## 4,800
Open access books available

## 122,000
International authors and editors

## 135M
Downloads

Our authors are among the

## 154
Countries delivered to

## TOP 1%
most cited scientists

## 12.2%
Contributors from top 500 universities

**BOOK CITATION INDEX**
CLARIVATE ANALYTICS
INDEXED

**WEB OF SCIENCE**™

Selection of our books indexed in the Book Citation Index
in Web of Science™ Core Collection (BKCI)

# Interested in publishing with us?
# Contact book.department@intechopen.com

Numbers displayed above are based on latest data collected.
For more information visit www.intechopen.com

# Pressure Drop and Heat Transfer during a Two-phase Flow Vaporization of Propane in Horizontal Smooth Minichannels

Jong-Taek Oh, Kwang-Il Choi and Nguyen-Ba Chien

## 1. Introduction

Nowadays, the ozone depletion and global warming potential of commonly used refrigerant have been considered as a major environmental matter. The next generation of refrigerants is obliged, not only to be environment friendly, but also to provide high efficiency [1]. Therefore, considerable attention has been focused on the application of natural refrigerant. However, safety issues have been established, such as special demands or suitable applications for refrigerants which include high working pressure, flammability, or toxicity.

Propane is a natural refrigerant that has no ODP and low GWP. It is also a non-toxic chemical and has a suitable thermodynamics and a transport property which are almost similar with those of HFC refrigerant. Other advantages of propane include compatibility with most materials used in HFC equipment and miscibility with commonly used compressor lubricant. The HFC systems such as R22 one can use propane without major changes. Nonetheless, propane has a high flammability that meets the safety demands of refrigerants in design and operation. It means that the propane refrigeration systems should work with minimum refrigerant charges and zero refrigerant leakage.

The question now is: "Could the refrigeration systems avoid leakage?" The answer comes from the difference between the design and the actual, which is a challenge. Mobile air conditioning and commercial refrigerant systems are two types of those that have the largest amount of leakage. The estimated leakage rates of these systems are 7% and 15-20% of the total charges, respectively [2]. Although the leakage percentage improves every year through the development of technology, it is still high and could not possibly reach the ideal case in the near future. The fact clearly shows that the designs of propane systems currently need a decrease in the

amount of refrigerant charges to as minimal as possible. And one of the best solutions at present is the decrease in the size of the heat exchanger. Compact heat exchangers using minichannels and microchannels have more efficient heat transfer performance than conventional types, due to their higher heat transfer area per refrigerant volume. Given that, the systems could reduce the refrigerant changers but still keep the coefficient of performance. However, since various researches observed the many differences of heat transfer and pressure drop of refrigerants in the mini/microchannels and conventional channels [3, 4]. The studies on these characteristics of propane in mini/microchannels and valuable information will be provided for researchers in related fields.

In fact, in the past few decades, numerous interesting researches were published in literature such as the studies of [5-9]. Nevertheless, the following chapter does not attempt to review all the available literature but those most focused on the particular heat exchanger design only or the consideration on the heat transfer and pressure drop separately. The intention is to rather present a basis on heat transfer and pressure drop of propane in minichannels, simultaneously under the variation of mass fluxes, heat fluxes, saturated temperature, and tube diameter. The phenomenon will be explained thoroughly by its mechanism that shows some differences observed in the conventional channel. Furthermore, the development of heat transfer coefficient and pressure drop correlations are demonstrated. The content is believed to bring up the general understanding, as well as useful information on heat exchanger designs to the readers.

## 2. Experimental apparatus and data reduction

### 2.1. Experimental model

The schematic diagram of experimental apparatus is depicted in Fig. 1. The facilities were built by Choi et al. [6]. Looking inside, the model mainly comprises the condensing unit, sub-cooler, receiver, pump, mass flow meter, preheater, and test section. The closed refrigeration cycle starts from the receiver. The liquid refrigerant was, at first, pumped by a magnetic gear pump. Then, it was passed through a Coriolis mass flow meter. Before entering the test section, the mass quality of the refrigerant was adjusted by the preheater. At the test section, it was evaporated by applying heat from an AC transformer. The vapor refrigerant at the outlet of the test section was condensed by the condenser and then the liquid refrigerant comes back to the receiver. In this model, the flow rate of the refrigerant can be acquired by controlling the frequency of the gear pump. The photograph of the apparatus is presented in Fig. 2.

The test section was made of stainless steel smooth tube with inner diameters of 1.5mm and 3.0 mm and heated lengths of 1000mm and 2000 mm, respectively. The temperatures of the outside surface of the test section were measured at the top, on both sides, and at the bottom each at 100mm axial intervals from the inlet to the outlet. In this model, Choi et al. [6] used the T-type thermocouples with the outside diameter of 0.1mm. To measure the local pressure in the test section, two pressure gauges were set up at the inlet and outlet. Another differential pressure was used to estimate the exact pressure drop during the evaporation in the test tube. Two sight glasses with the same inner diameter as the test section were installed to visualize
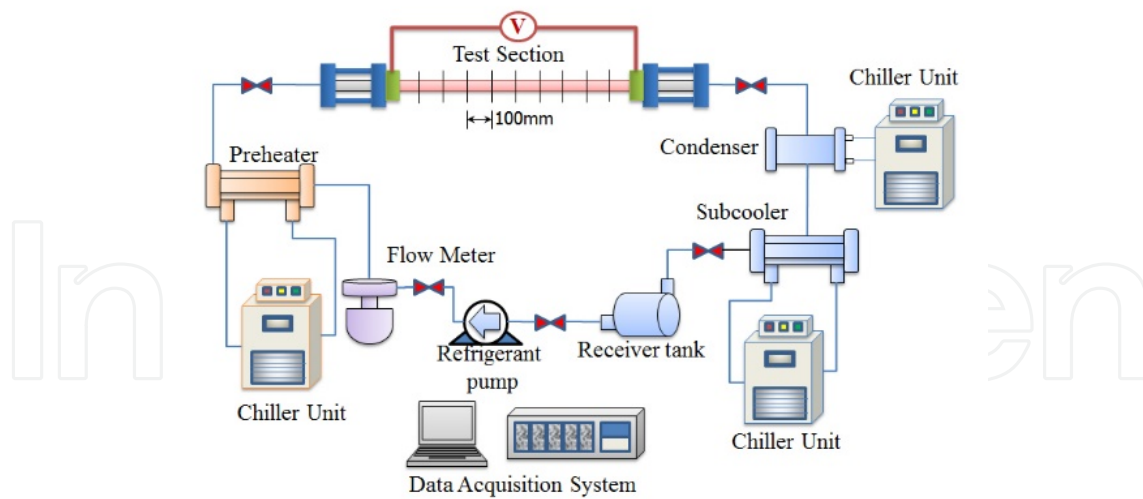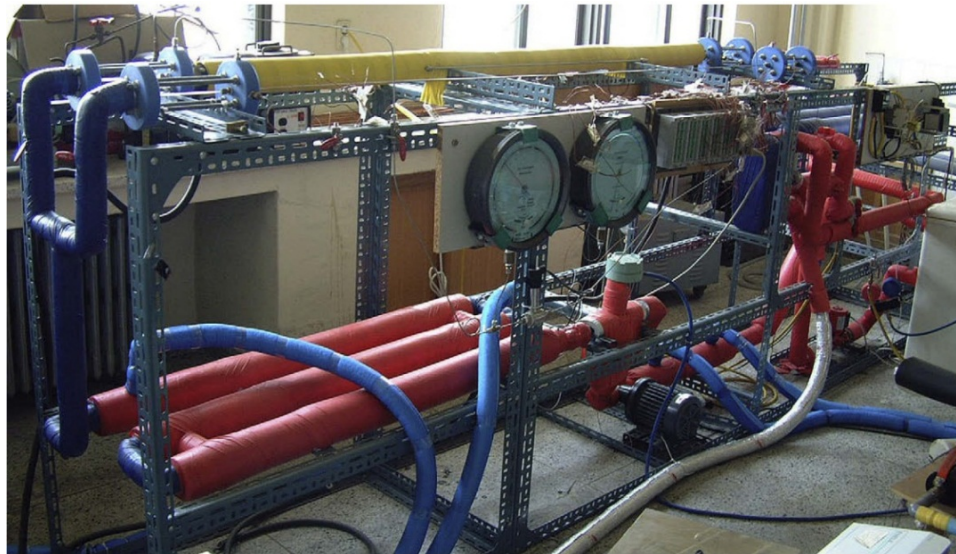
**Figure 1.** The schematic of apparatus



**Figure 2.** The Photograph of apparatus

the flow. After all, the test sections and the other components were well isolated by rubber and foams to reduce the effect of the environment. The details of the test section are depicted in Fig. 3.

One of the most important parts in this testing model is to test the heat balance on a test tube. The total electric power was calculated by the root mean square values of electric voltage and current. The heat balance procedure was taken with each tube. The results were then corrected by using logarithmic regression method. The final deviation of electric power was within 5%. The estimated uncertainties of other parameters were also evaluated with the confidence of 95%. The summary is shown in table 1. The testing conditions in study of Choi et al. [6] were also illustrated in table 2. All the properties of refrigerant were queried from REFPROP. 8.

## 2.2. Data reduction

### 2.2.1. Pressure drop

The total pressure drop of saturated refrigerants comes from the variation of kinetic energy, potential energy, and the friction of the two-phase flow on the wall. In horizontal tubes, the potential energy can be neglected, thus, the total pressure drop is the sum of the momentum pressure drop and the frictional pressure drop. Assuming that the pressure drop linearly increases with the tube length, the saturation pressure at the starting point of saturation regime is interpolated from the measured pressure and the calculated subcooled length. The experimental two phase frictional pressure drop can be determined as follows:

$$\left(-\frac{dp}{dz}F\right) = \left(-\frac{dp}{dz}\right) - \left(-\frac{dp}{dz}a\right) \tag{1}$$

The refrigerant is evaporated from liquid at the saturation temperature to vapor-liquid mixture at mass quality x with a linear change of test distance over the tube length. Hence, the momentum pressure drop can be calculated with following equation:

$$\left(-\frac{dp}{dz}a\right) = G^2 \frac{d}{dz}\left(\frac{x^2}{\alpha \rho_g} + \frac{(1-x)^2}{(1-\alpha)\rho_f}\right) \tag{2}$$

Choi et al. [6] compared various void fraction models including the ones proposed by Steiner [10], CISE [11], and Chisholm [12] with the homogeneous model and their experimental data. The correlation proposed by CISE shows the best agreement with the homogeneous model, while Steiner's correlation shows the best prediction for the experimental data as shown in Fig. 4. Therefore, the void fraction in their study is obtained from the Steiner [10] void fraction as follows:

$$\alpha = \frac{x}{\rho_g}\left[(1+0.12(1-x))\left(\frac{x}{\rho_g} + \frac{1-x}{\rho_f}\right) + \frac{1.18(1-x)\left[g\sigma(\rho_f - \rho_g)\right]^{0.25}}{G\rho_f^{0.5}}\right]^{-1} \tag{3}$$

The friction factor was determined from the measured pressure drop for a given mass flux by using the Fanning equation,

$$f_{tp} = \frac{D_{\bar{\rho}}}{2G^2}\left(-\frac{dp}{dz}F\right) \tag{4}$$

where the average density is calculated with the following equation:

$$\bar{\rho} = \alpha \rho_g + (1-\alpha)\rho_f \qquad (5)$$

The two phase frictional multiplier, $\phi_{fo}^2$, is determined by dividing the calculated frictional two-phase pressure drop to the pressure drop of the liquid flow assuming the total flow to be liquid. The equation is defined as:

$$\phi_{fo}^2 = \left(-\frac{dp}{dz}F\right)_{tp} \Big/ \left(-\frac{dp}{dz}F\right)_{fo} = \left(-\frac{dp}{dz}F\right)_{tp} \Big/ \left(\frac{2f_{fo}G^2}{D\rho_f}\right) \qquad (6)$$
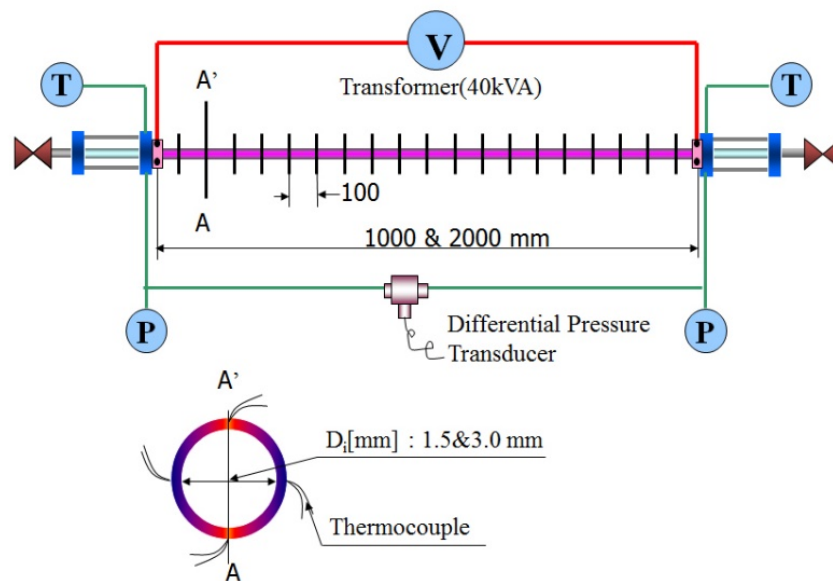


**Figure 3.** The schematic of test sections

| Test section | Horizontal stainless steel circular smooth small tubes |
| --- | --- |
| Quality | Up to 1.0 |
| Working refrigerant | Propane |
| Inlet diameter (mm) | 1.5 and 3.0 |
| Tube length (mm) | 1000 and 2000 |
| Mass flux (kg m$^{-2}$ s$^{-2}$) | 50-400 |
| Heat flux(KW m$^{-2}$) | 5-20 |
| Inlet T$_{sat}$ (℃) | 0, 5, 10 |

**Table 1.** Experimental Conditions

| Parameter | Uncertainty at a 95% confidence level |
|---|---|
| *Thermocouples* (°C) | ±0.62 |
| *P* (kPa) | ±2.5 |
| *G* (%) | ±5.89 |
| *q* (%) | ±2.54 |
| *x* (%) | ±6.21 |
| *h*(%) | ±6.89 |

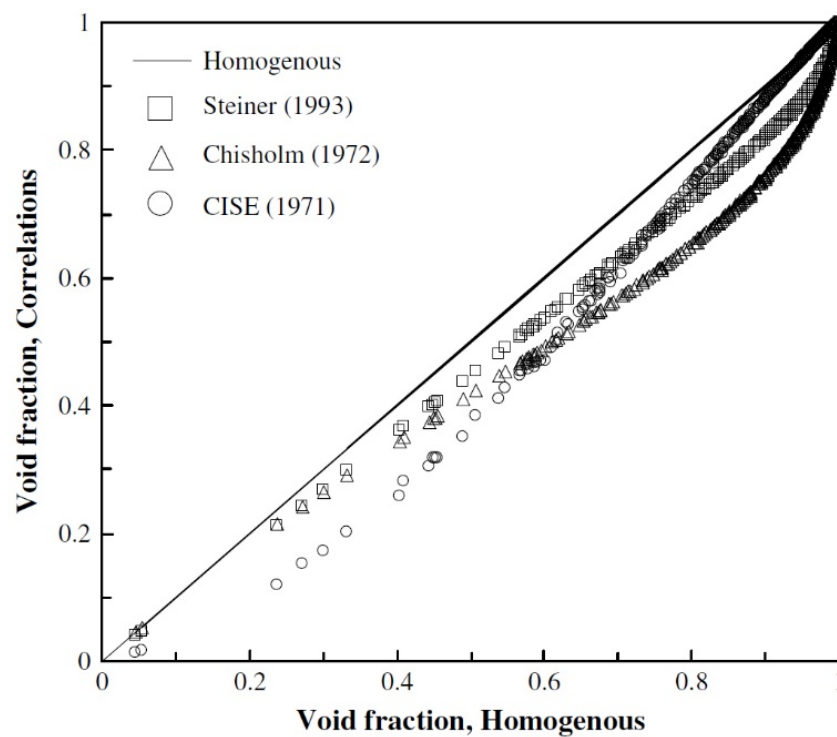**Table 2.** Summary of the estimated uncertainty



**Figure 4.** Void fraction comparison between the homogenous model and the existing correlations

### 2.2.2. Heat transfer coefficient

Choi et al. [6] determined the inside tube wall temperature, $T_{wi}$, by the average inside temperature of the top, both right and left sides, and bottom wall temperatures. As demonstrated in the apparatus module, the heat was applied on test tubes through uniform current, and the local temperature was evaluated at the cross section where there is an attached the thermocouple, hence, the inside wall temperatures at each point could be determined by using steady state one-dimensional radial conduction heat transfer through the wall with internal heat generation. The quality, x, at the measurement location, z, was determined based on the thermodynamic properties.

$$x = \frac{i - i_g}{i_{fg}} \tag{7}$$

In fact, the refrigerant flow was not completely saturated at the inlet of the test section. The flow becomes totally saturated after a short initial length of tube when the heat, which is called a subcooled length, was applied. Therefore, to ensure the accuracy of data reduction, the subcooled length is calculated using the following equation:

$$z_{sc} = L \frac{i_f - i_{fi}}{\Delta i} = L \frac{i_f - i_{fi}}{(Q/W)} \tag{8}$$

The outlet mass quality was then determined using the following equation:

$$x_o = \frac{\Delta i + i_{fg} - i_f}{i_{fg}} \tag{9}$$

## 3. Results and discussion

### 3.1. Two-phase flow pressure drop

The study of Choi et al. [6] showed that mass flux, heat flux, inner tube, and saturation temperature all have affected the two-phase flow pressure drop of propane in minichannels. The effect of mass flux on the pressure drop is shown in Fig. 5. It can be seen that the mass flux has a strong influence on the pressure drop. As described above, the two-phase pressure drop is mainly caused by the frictional and acceleration pressure drop. The increase in the mass flux results in a higher flow velocity, which increases both of the two components and, therefore, increases the pressure drop. The similar trends were reported in the studies [13-17]. The strong effect of heat flux on the pressure drop is also described in Fig. 5. An increase in the heat flux causes a higher vaporization. The average vapor quality and flow velocity of higher heat flux conditions increase faster than those of lower ones, and lead to the increase of the pressure drop when the heat flux increases. The results were in well agreement with the study of Zhao et al. [13]. In addition, Fig. 5 illustrates the effect of the tube diameter on the pressure drop. The comparison of the pressure gradient with the inner diameter of 1.5 and 3.0 mm shows that it is higher in smaller diameter. This phenomenon can be explained by saying that the wall shear stress is higher in smaller tubes, which results in both higher frictional and acceleration pressure drop. The effect of saturation temperature on the pressure drop is also observed in Fig. 5. The pressure gradient is higher at a lower saturation temperature. The physical properties are believed to be the reason for this phenomenon. The liquid density and the viscosity of propane increase when the saturation temperature decreases. Hence, at the constant mass flux conditions, the liquid velocity becomes lower, while the vapor velocity is higher. This means the pressure drop increases during evaporation as the saturation temperature decrease.
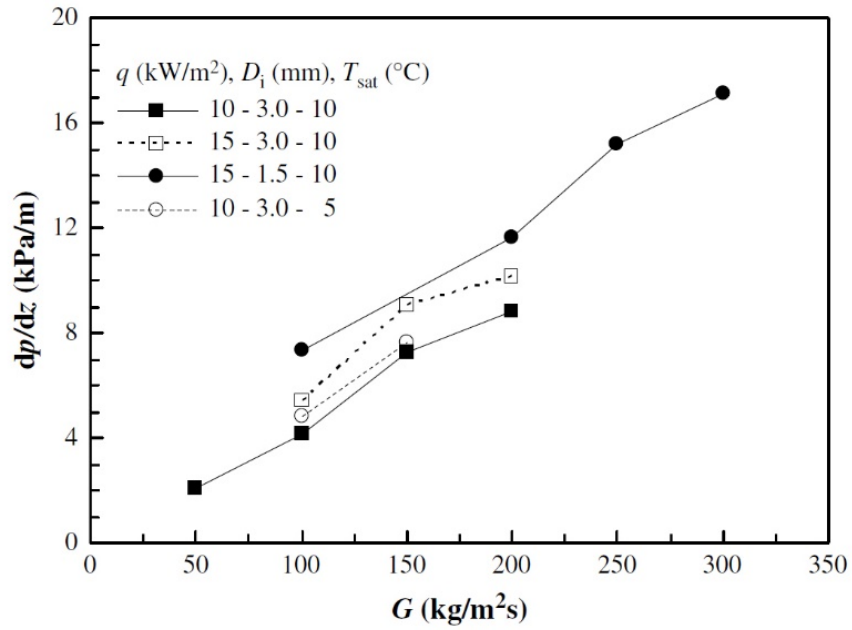
**Figure 5.** The effect of mass flux, heat flux, inner tube diameter and saturation temperature on the pressure drop
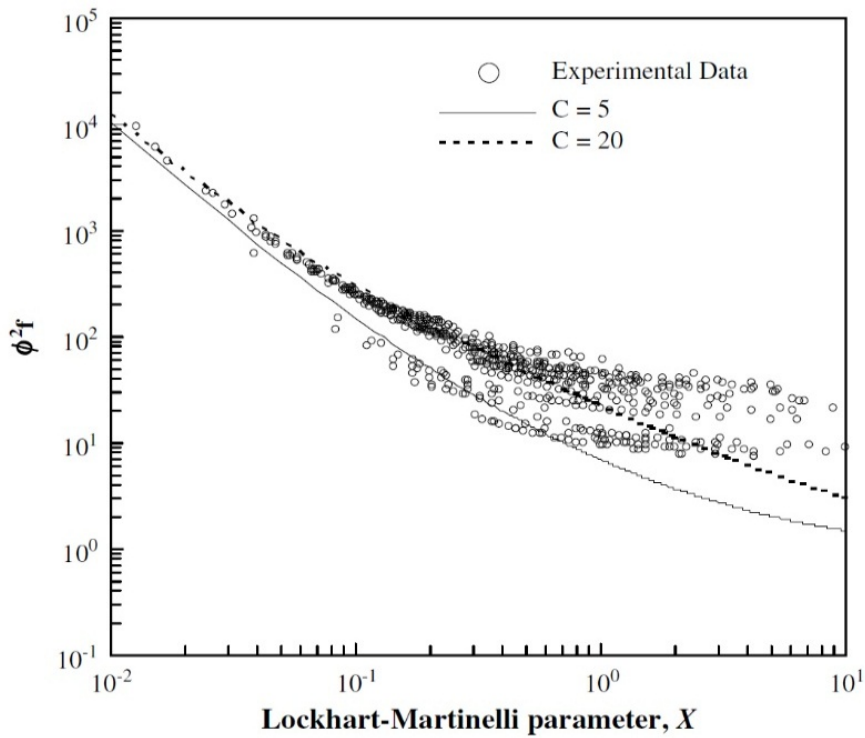


**Figure 6.** Variation of the two-phase frictional multiplier data with the Lockhart-Martinelli parameter

The comparison of the two-phase frictional multiplier data with the value was predicted from the Lockhart Martinelli correlation with C factors equal to 5 and 20. The value of factor Cs was evaluated follow the study of Chisholm [18]. As shown in figure 6, the presented data is distributed in all regimes: under the baseline C = 5, upper the baseline C = 20, and between the two baselines. That means the flow characteristics include laminar, co-current laminar-turbulent, and turbulent flows were observed in the data.

In order to validate the experimental data, the frictional pressure drop of propane was compared with the 13 existing correlations [19 – 31] as shown in Table 3. Among them, the correlations of Mishima and Hibiki [19], Friedel [20] and Chang et al. [21] showed the best prediction with the experimental data. Mishima and Hibiki [19] proposed the frictional pressure drop for air-water in the vertical tube with an inner diameter of 1 to 4 mm, based on the Chisholm's equation. Before that time, using a large database, the model developed by Friedel [20] can be used to predict the frictional pressure drop in both the horizontal and vertical upward flow. The correlation of Chang et al. [21] was developed with the data of R410A and air-water in a 5mm smooth tube. Other correlations, including 4 homogenous models proposed, showed large mean deviations.

| Pressure drop correlations | Deviation (%) | |
|---|---|---|
| | Mean | Average |
| Mishima and Hibiki [19] | 35.37 | -25.08 |
| Friedel [20] | 38.79 | -21.91 |
| Chang et al. [21] | 38.86 | -21.99 |
| Cicchitti et al. [22]-homogeneous | 48.67 | -40.27 |
| Beattie and Whalley [23]-homogeneous | 54.68 | -51.69 |
| McAdams [24]-homogenous | 56.07 | -53.73 |
| Dukler et al. [25]-homogeneous | 58.75 | -57.32 |
| Lockhart and Martinelli [26] | 41.36 | 3.46 |
| Chisholm [27] | 45.24 | 18.00 |
| Zhang and Webb [28] | 46.82 | 7.58 |
| Chen et al. [29] | 63.67 | -63.60 |
| Kawahara et al. [30] | 73.04 | -72.92 |
| Tran et al. [31] | 77.99 | 35.60 |

**Table 3.** Deviation of the pressure drop comparison between the present data and the previous correlations.

| | |
|---|---|
| Lockhart and Martinelli [26] | $\phi_f^2 = 1 - \dfrac{C}{X_{tt}} + \dfrac{1}{X_{tt}^2};$ <br><br> $X_{tt} = \left(\dfrac{1-x}{x}\right)^{0.9}\left(\dfrac{\rho_g}{\rho_f}\right)^{0.5}\left(\dfrac{\mu_f}{\mu_g}\right)^{0.1}; \, C_{turbulent-turbulent} = 20$ |
| Friedel [20] | $\phi_{fo}^2 = (1-x)^2 + x^2[(\rho_f f_{go})/(\rho_g f_{fo})] + 3.24 A_2 A_3 Fr^{-0.045} We^{-0.035}$ <br><br> $A_2 = x^{0.78}(1-x)^{0.224}$ <br><br> $A_3 = \left(\dfrac{\rho_f}{\rho_g}\right)^{0.91}\left(\dfrac{\mu_f}{\mu_g}\right)^{0.19}\left[1-\left(\dfrac{\mu_f}{\mu_g}\right)\right]^{0.7}$ |

Chisholm [27]

$\phi_{fo}^2 = 1 + (\Gamma^2 - 1)[Bx^{0.875}(1-x)^{0.875} + x^{0.175}]$

$\Gamma^2 = \left(\dfrac{dp}{dz}\right)_{go} \Big/ \left(\dfrac{dp}{dz}\right)_{fo}$

| $\Gamma$ | $G\,(kg\,m^{-2}s^{-1})$ | B |
|---|---|---|
| $\leq 9.5$ | $\leq 500$ | 4.8 |
| | $500 < G < 1900$ | $2400/G$ |
| | $G \geq 1900$ | $55/G^{0.5}$ |
| $9.5 < \Gamma < 28$ | $\leq 600$ | $520/(\Gamma G^{0.5})$ |
| | $> 600$ | $21/\Gamma$ |
| $\geq 28$ | - | $\Gamma^2 G^{0.5}$ |

| | |
|---|---|
| Mishima and Hibiki [19] | $\phi_f^2 = 1 - \dfrac{C}{X_{tt}} + \dfrac{1}{X_{tt}^2}$ <br><br> $X = \left(-\dfrac{dp}{dz}F\right)_f \Big/ \left(-\dfrac{dp}{dz}F\right)_g$ <br><br> $C = 21(1 - e^{-319 \times 10^{-6}})$ |
| Tran et al. [31] | $\phi_{fo}^2 = 1 + (4.3\Gamma^2 - 1)\left(N_{conf} x^{0.875} + x^{1.75}\right)$ <br><br> $\Gamma^2 = \dfrac{\left(\dfrac{dp}{dz}\right)_{go}}{\left(\dfrac{dp}{dz}\right)_{fo}}; \, N_{conf} = \dfrac{\left[\dfrac{\alpha}{g(\rho_f - \rho_g)}\right]^{0.5}}{D}$ |
| Zhang and Webb [28] | $\phi_{fo}^2 = (1-x)^2 + 2.87x^2\left(\dfrac{P}{P_c}\right)^{-1} + 1.68x^{0.8}(1-x)^{0.25}\left(\dfrac{P}{P_c}\right)^{-1.64}$ |

**Table 4.** Summary of some correlations of two-phase flow pressure drops.

## 3.2. Heat transfer coefficient

The mass flux, heat flux, inner tube, and saturation temperature also have affected the two-phase flow boiling heat transfer coefficient of propane in the minichannels. Fig. 7 shows the effect of mass flux on heat transfer coefficient. No significant effect of mass flux on the heat transfer coefficient was observed in the low quality region. This phenomenon indicates that the nucleate boiling heat transfer is predominant. The similar tendency of nucleate boiling was performed in numerous studies by Kew and Cornwell [32], Lazarek and Black [33], Wambsganss et al. [34], Tran et al. [35], and Bao et al. [36], those that used small tubes. The dominant of nucleate boiling heat transfer occurred due to the effect of small channels and the physical properties of the refrigerant. The heat transfer coefficient is higher with higher heat flux at high quality regime since the development of convective boiling heat transfer. The trend also depicts that the drop of heat transfer coefficient appears sooner in higher mass flux. The flow pattern develops faster in the smaller tube and higher mass flux, which lead to the occurrence of dry patches at lower quality.
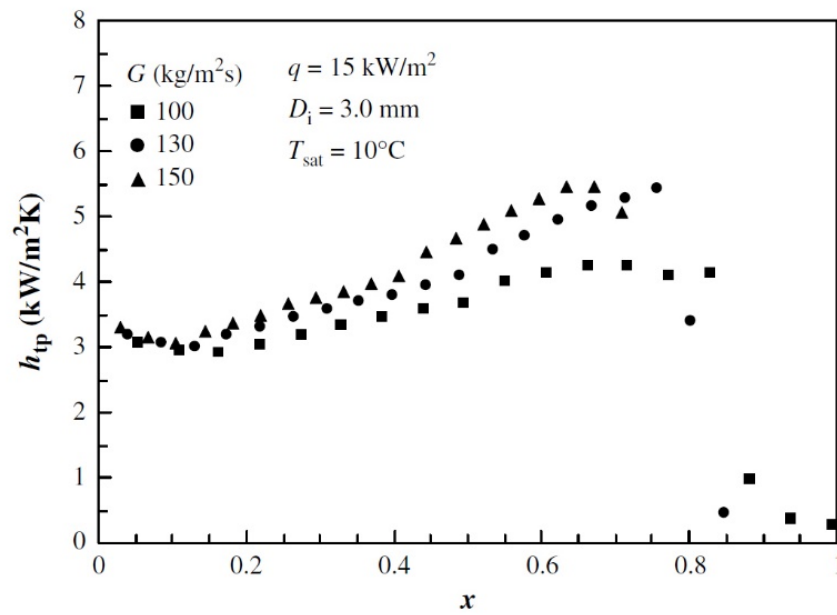
**Figure 7.** The effect of mass flux on heat transfer coefficient

The influence of heat flux on the heat transfer coefficient is illustrated in Fig. 8. The strong effect of heat flux is observed at a low quality regime. It means that the nucleate boiling heat transfer contribution is dominant. When the vapor quality increases, the nucleate boiling heat transfer is suppressed. Therefore, the effect of heat flux becomes limited. The heat transfer coefficient increases continuously in high quality regime, but no difference is found in given conditions. It shows that the convective boiling heat transfer contribution is predominant in this regime.
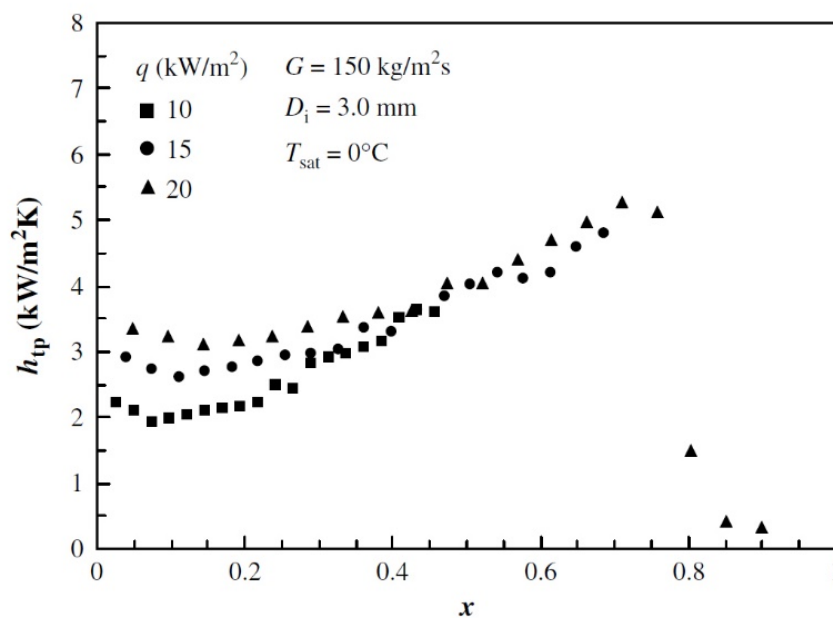


**Figure 8.** The effect of heat flux on heat transfer coefficient

Fig. 9 shows the effect of a tube diameter on the heat transfer coefficient of propane. The heat transfer coefficient is higher in a smaller tuber diameter at a low quality regime. It can be explained that the nucleate boiling is more active when the tube diameter decreases. In addition, the heat transfer performance is higher in smaller tubes at given conditions due to the increase in contact surface per refrigerant volume.
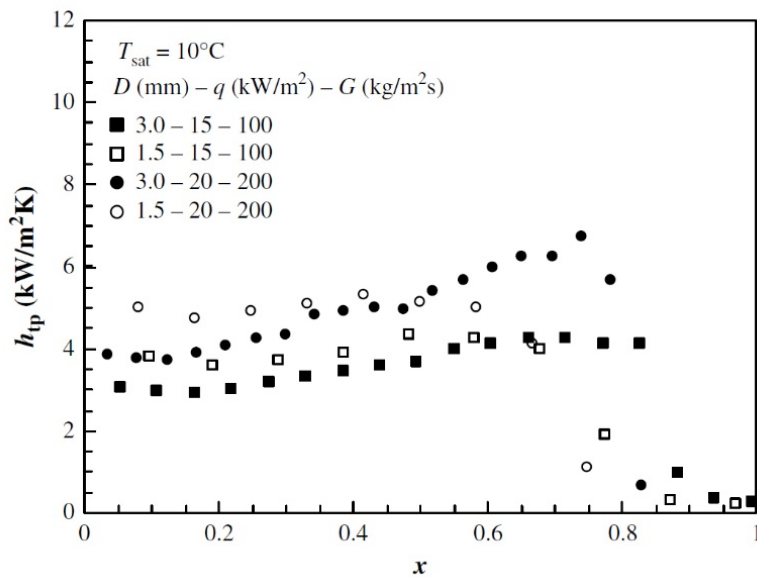


**Figure 9.** The effect of inner tube diameter on heat transfer coefficient

Fig. 10 illustrates the effect of saturation temperature on the heat transfer coefficient. The increase in saturation temperature leads to the increase in heat transfer coefficient. The reason is that the surface tension is lower and the saturation temperature is higher when the saturation pressure increases. Hence, the heat transfer coefficient is higher when it is considered during the vapor formation in the boiling process.



**Figure 10.** The effect of saturation temperature on heat transfer coefficient

## 4. Development of new correlations

### 4.1. Pressure drop correlation

The accuracy of predicting two-phase flow pressure drops in heat exchanger devices is quite important in the design and performance optimization of 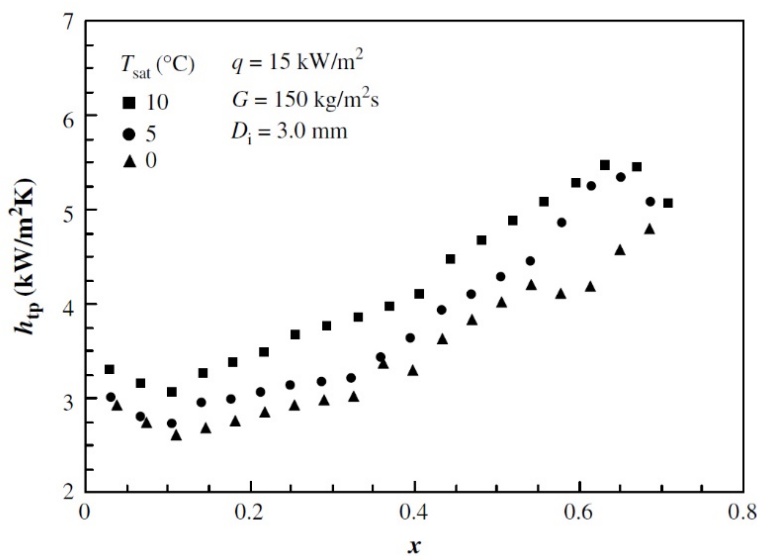refrigeration systems. For a simple example, if the predicting method shows a higher value compared to the real value, the material design will cost higher. While, on the other hand, if the predicting value is lower than the real value, the performance of the design system would not reach the estimated values. In addition, the comparison of experimental pressure drops of propane and existing correlations described above showed high deviations. Hence, a more precise pressure drop correlation was proposed by Choi et al [6]. The new correlation was developed based on the method of Lockhart and Martinelli [26]. The pressure drop model of Lockhart and Martinelli [26] is defined in the basis pressure drop of three terms including the liquid phase, vapor phase, and the interaction between two phases. The ideal can be expressed in the following equation:

$$\left(-\frac{dp}{dz}F\right)_{tp} = \left(-\frac{dp}{dz}F\right)_{f} + C\left[\left(-\frac{dp}{dz}F\right)_{f}\left(-\frac{dp}{dz}F\right)_{g}\right]^{1/2} + \left(-\frac{dp}{dz}F\right)_{g} \tag{10}$$

The two-phase frictional multiplier based on the pressure gradient for the liquid alone flow, $\phi_f^2$, is calculated by dividing Eq.(10) by the liquid phase pressure drop, as is shown in Eq. (11).

$$\phi_f^2 = \frac{\left(-\frac{dp}{dz}F\right)_{tp}}{\left(-\frac{dp}{dz}F\right)_{f}} = 1 + C\left[\frac{\left(-\frac{dp}{dz}F\right)_{g}}{\left(-\frac{dp}{dz}F\right)_{f}}\right]^{1/2} + \frac{\left(-\frac{dp}{dz}F\right)_{g}}{\left(-\frac{dp}{dz}F\right)_{f}} = 1 + \frac{C}{X} + \frac{1}{X^2} \tag{11}$$

The Martinelli parameter, X, is defined by the following equation:

$$X = \left[\frac{\left(-\frac{dp}{dz}F\right)_{f}}{\left(-\frac{dp}{dz}F\right)_{g}}\right]^{1/2} = \left[\frac{2f_fG^2(1-x)^2\rho_g/D}{2f_gG^2x^2\rho_f/D}\right]^{1/2} = \left(\frac{f_f}{f_g}\right)^{1/2}\left(\frac{1-x}{x}\right)\left(\frac{\rho_g}{\rho_f}\right)^{1/2} \tag{12}$$

The friction factor in Eq. (12) was determined by the flow conditions: laminar (for Re < 1000), $f = 16\text{Re}^{-1}$, or turbulent (for Re > 2000), $f = 0.079\text{Re}^{-0.25}$. For the transition regime, the frictional factor was calculated by interpolating the equations of two regimes.

As discussed in the section above, the experimental result showed that the pressure drop is a function of mass flux, inner tube diameter, surface tension, density, and viscosity. Therefore

Choi et al. [6] proposed the factor C in Eq. (11) as a function of the two-phase Weber number, $We_{tp}$, and the two-phase Reynolds number, $Re_{tp}$. A new factor C was developed using the regression method, as shown in Eq. (13).

$$C = \left( \phi_f^2 - 1 - \frac{1}{X^2} \right) X = 1732.953 \times Re_{tp}^{-0.323} We_{tp}^{-0.24} \tag{13}$$

Fig. 11 illustrates the two-phase frictional multiplier comparison between the propane experimental data and the prediction with the new correlation proposed by Choi et al. [6]. The comparison shows a mean deviation of 10.84% and an average deviation of 1.08%.
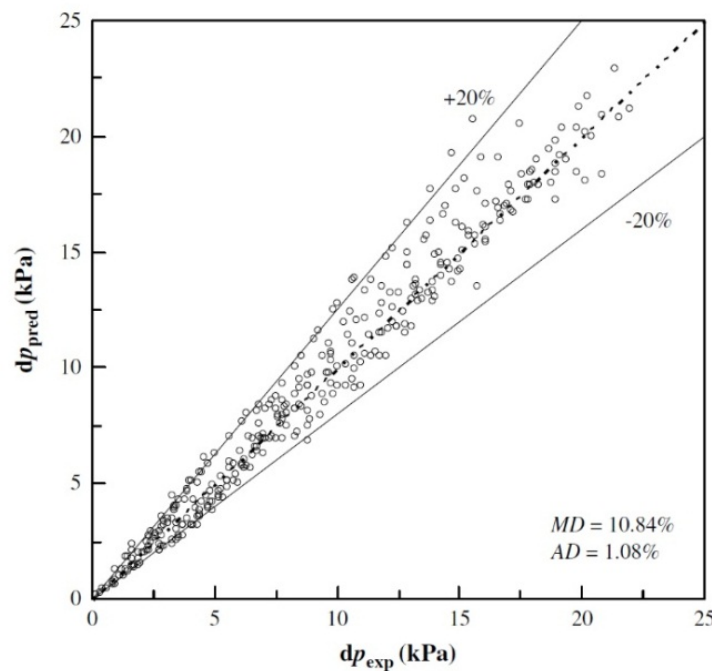


**Figure 11.** Comparison of the experimental and predicted pressure drop using the new developed correlation

## 4.2. Heat transfer coefficient correlation

Choi et al. [6] have compared the experimental heat transfer coefficents of propane with the nine correlations for boiling heat transfer coefficient, as shown in tables 5 and 6. The Shah [37] and Tran et al. [35] correlations provided the better prediction among the other presented correlations. The correlation developed by Shah [37] used a large databank from 19 independent studies with various fluids. The correlation can be used to predict the heat transfer coefficient in both horizontal and vertical tubes. However, this correlation was developed for conventional tubes. Tran et al. [35] proposed a nucleation-dominant form of heat transfer coefficient correlation based on the data of R-12 and R-113 in small circular and rectangular channels. Other correlations include the ones proposed by Jung et al. [38], Gungor and

Winterton [39], Takamatsu et al. [40], and Kandlikar and Steinke [41], where the mean deviation is around 30%. The Gungor–Winterton's correlation [39] was a modification of the superposition model; it was developed using some fluids in several small and conventional channels with various test conditions. The correlations proposed by Wattelet et al. [42] and Chen [43] showed a large mean deviation, since both of them were developed for large tube diameters. The correlation proposed by Zhang et al. [44] used the data of some working fluids without any hydrocarbon, hence, couldn't predict the present data well. The above comparisons showed the need of developing a more accurate heat transfer coefficient correlations. Based on the one proposed by Chen [43], Choi et al. [6] developed a new correlation for the two-phase flow boiling of propane. He noted that the correlation only used the experimental data prior to the dry-out.

It is well known that the flow boiling heat transfer is mainly governed by the following two important mechanisms: nucleate boiling and forced convective evaporation. The basic form is described by Chen [43] as follows:

$$h_{tp} = F.h_{conv} + h_{nb}.S \tag{14}$$

The convective component was also presented by a Dittus-Boelter type equation.

$$h_{lo} = 0.023 \left[ \frac{G(1-x)D}{\mu_f} \right]^{0.8} \left[ \frac{\mu_f c_p}{k_f} \right]^{0.4} \frac{k_f}{D} \tag{15}$$

| Heat transfer coefficient correlations | Deviation (%) | |
|---|---|---|
| | Mean | Average |
| Chen [43] | 50.82 | 18.74 |
| Gungor and Winterton [39] | 28.44 | 23.78 |
| Shah [37] | 19.21 | 3.55 |
| Takamatsu et al. [40] | 32.69 | 32.15 |
| Wattelet et al. [42] | 48.28 | 48.28 |
| Tran et al. [35] | 21.18 | -6.15 |
| Kandlikar and Steinke [41] | 33.84 | 24.41 |
| Zhang et al. [44] | 79.21 | 77.89 |
| Jung et al. [38] | 26.05 | 23.38 |

**Table 5.** Deviation of the heat transfer coefficient comparison between the present data and the previous correlations.

| Chen [43] | $h_{tp} = S.h_{nb} + F.h_{lo}; where: S = fn(\text{Re}_{tp}); F = fn(X_{tt})$ <br><br> $h_{nb} = 0.00122 \left[ \dfrac{k_f^{0.79} c_{pf}^{0.45} \rho_f^{0.49}}{\sigma^{0.5} \mu_f^{0.29} i_{fg}^{0.24} \rho_g^{0.24}} \right] \Delta T_e^{0.24} \Delta p_e^{0.75}; h_{lo} = 0.023 \left[ \dfrac{G(1-x)D}{\mu_f} \right]^{0.8} \left[ \dfrac{\mu_f c_p}{k_f} \right]^{0.4} \dfrac{k_f}{D}$ |
|---|---|
| Gungor and Winterton [39] | $h_{tp} = E_{new} \times h_l$ <br><br> $E_{new} = 1 + 3000 Bo^{0.86} + 1.12 \left( \dfrac{x}{1-x} \right)^{0.75} \left( \dfrac{\rho_l}{\rho_v} \right)^{0.41}$ <br><br> If the tube is horizontal and the Froude number $(Fr_l)$ is less than 0.05 then E should be multiplied by the factor $E_2 = Fr_l^{(0.1-2Fr_l)}$ |
| Shah [37] | $\psi = \dfrac{h_{TP}}{h_f}; Co = \left( \dfrac{1}{x-1} \right)^{0.8} \left( \dfrac{\rho_g}{\rho_f} \right)^{0.5}; Bo = \dfrac{q}{Gh_{fg}}; Fr_f = \dfrac{G^2}{\rho_f^2 gD}$ <br><br> $h_l = 0.023 \text{Re}_f^{0.8} \text{Pr}_f^{0.4} \left( \dfrac{k_f}{D_f} \right)$ |
| Jung et al. [38] | $h_{tp} = S.h_{SA} + F.h_{lo}$ <br><br> $h_{SA} = 207 \dfrac{k_1}{bd} \left( \dfrac{qbd}{k_1 T_{sat}} \right)^{0.745} \left( \dfrac{\rho_g}{\rho_f} \right)^{0.581} \text{Pr}_f^{0.533};$ <br><br> $h_l = 0.023 \text{Re}_f^{0.8} \text{Pr}_f^{0.4} \left( \dfrac{k_f}{D_f} \right)$ <br><br> $bd = 0.0146 \left( \dfrac{35\pi}{180} \right) \left[ \dfrac{2\sigma}{g(\rho_f - \rho_g)} \right]^{0.5}$ <br><br> $S = 4048 X_{tt}^{1.22} Bo^{1.13} for: X_{tt} < 1$ <br><br> $F = 2.37 \left( 0.29 + \dfrac{1}{X_{tt}} \right)^{0.85}$ |
| Wattelet et al. [42] | $h_{tp} = \left[ h_{nb}^n + h_{cb}^n \right]^{1/2}; n = 2.5$ <br><br> $h_{nb} = 55 p_r^{0.12} (-0.4343 \ln p_r)^{-0.55} M^{-0.5} q^{0.67}$ <br><br> $h_{cb} = 0.023 \text{Re}_f^{0.8} \text{Pr}_f^{0.4} \left( \dfrac{k_f}{D_f} \right) \times F \times R$ <br><br> $F = fn(X_{tt}); and S = fn(\text{Re}_{tp})$ |
| Tran et al. [35] | $h = (8.4 x 10^{-5})(Bo^2 We_f)^{0.3} \left( \dfrac{\rho_f}{\rho_g} \right)^{-0.4}$ |
| Kandlikar and Steinke [41] | $\dfrac{h_{tp}}{h_f} = D_1 Co^{D_2} \left( \substack{1 x 0.8 \\ -} \right) fn(Fr_{fo}) + D_3 Bo^{D4} \left( \substack{1 x 0.8 \\ -} \right) Fn$ <br><br> $fn(Fr_{fo}) = 1$ |
| Zhang et al. [44] | $h_{tp} = S.h_{nb} + F.h_{sp}$ <br><br> $h_{nb} = 0.00122 \left[ \dfrac{k_f^{0.79} c_{pf}^{0.45} \rho_f^{0.49}}{\sigma^{0.5} \mu_f^{0.29} i_{fg}^{0.24} \rho_g^{0.24}} \right] \Delta T_e^{0.24} \Delta p_e^{0.75}$ <br><br> $h_{sp} = MAX(h_{Dittus-Boelter}) if \text{Re}_f < 2300; h_{sp} = (h_{Dittus-Boelter}) if \text{Re}_f \geq 2300$ <br><br> $S = fn(\text{Re}_f); F = fn(\phi_f)$ |

Takamatsu et al. [40]

$$h_{tp} = F.h_{lo} + S.h_{pb}$$

$$h_{lo} = 0.0116 Re_{lo}^{0.89} Pr_l^{0.4} \frac{k_l}{D_i}$$

$$F = \left(\begin{smallmatrix}12\\-X_{tt}^{-0.88}\end{smallmatrix}\right)$$

$$h_{pb} = \left[405 C_1 k_l \left\{\frac{g(\rho_l - \rho_v)}{2\sigma}\right\}^{0.5} \left(\frac{S.\Delta T.La}{k_l.T_{sat}}\right)^{0.745} \left(\frac{\rho_v}{\rho_l}\right)^{0.581} Pr^{0.533}\right]^{1/0.255}$$

$$S = C_2 \left(\frac{\rho_l c_{pl}}{\rho_v h_{fg}} T_{sat}\right)^{1.25} La.F.h_{lo} \Big/ k_l$$

$$La = \sqrt{\frac{2\sigma}{g(\rho_l - \rho_v)}}$$

$$C_1 = 1.35; C_2 = 3.3 \times 10^{-5}$$

**Table 6.** Summary of existing heat transfer coefficient correlations

In small channels, the contribution of force convective heat transfer normally occurs later than it does in conventional channels due to the high contribution of nucleate boiling. Therefore, the enhancement factor F, which describes the increase in the convective heat transfer when the vapor quality increases, should be physically evaluated again. Chen [43] first introduced the enhanced factor F as the function of Lockhart-Martinelli parameter $X_{tt}$, $F = fn(X_{tt})$. Zhang et al. [44], later, took the flow condition effect in the enhanced factor into account. They introduced the relationship $F = fn(\phi_f^2)$, where $(\phi_f^2)$ is a general form proposed by Chisholm [18], as shown in Eq. (11). The values of the Chisholm parameter, C, are 20, 12, 10, and 5 corresponding to the four flow conditions of liquid and vapor: turbulent–turbulent (tt), laminar–turbulent (vt), turbulent–laminar (tv) and laminar–laminar (vv). However, as seen in the evaluation of existing heat transfer correlation above, the correlation of Zhang et al. [44] shows a large deviation with the present data. Hence, the factor F needs to reform to fit in the data.

Choi et al. [6] modified the enhancement factor F as a function of $(\phi_f^2)$, $F = fn(\phi_f^2)$, where $(\phi_f^2)$ is obtained from Eq. (11) - (13). The value of C in study of Choi et al. [6] is calculated by an interpolation of the Chisholm parameter with thresholds of Re = 1000 and Re = 2000 for the laminar and turbulent flows, respectively. On the other hand, the enhancement factor F must be reduced to 1 for pure liquid or pure vapor, and be greater than 1 within the two-phase regime. Hence, using a regression method, the formula of F is satisfied as follows:

$$F = MAX(0.5\phi_f, 1) \tag{16}$$

A new factor F is shown in Fig. 12.

Cooper [45] developed a correlation that used a large nucleate boiling data bank. Kew and Cornwell [32] and Jung et al. [46] showed that the Cooper [45] pool boiling correlation best predicted their experimental data. Therefore, the prediction of the nucleate boiling heat transfer for the present experimental data used Cooper [45], which is a pool boiling correlation developed based on an extensive study,

$$h = 55 p_r^{0.12} \left(-0.4343 \ln p_r\right)^{-0.55} M^{-0.5} q^{0.67} \qquad (17)$$

To account for the suppression of the nucleate boiling when vapor quality increases, Chen [43] defined the nucleate boiling suppression factor S, which is the ratio of mean superheat temperature, $\varDelta T_e$, to the wall superheat temperature, $\varDelta T_{sat}$. Jung et al. [38] introduced the suppression factor N as the function of $X_{tt}$ and boiling number, Bo, to take into account the strong effect of nucleate boiling in flow boiling. On the other hand, to consider the effect of flow conditions, the Lockhart – Martinelli parameter $X_{tt}$ is replaced by the two-phase frictional multiplier, $\phi_f^2$. Using the regression program and the experimental data, a new nucleate boiling suppression factor was proposed by Choi et al. [6]. It is as follows:

$$S = 181.458 \left(\phi_f^2\right)^{0.002} Bo^{0.816} \qquad (18)$$

The new heat transfer coefficient correlation is developed using 461 data points. Fig. 13 shows the comparison of the experimental heat transfer coefficient and the predicted one. The new correlation archives a good prediction with a mean deviation of 9.93% and an average deviation of -2.42%. When the C factor of the Chisholm [18] method is used to obtain $\phi_f^2$ for equations (11) and (16), the heat transfer coefficient also showed a good comparison mean deviation of 14.40%.
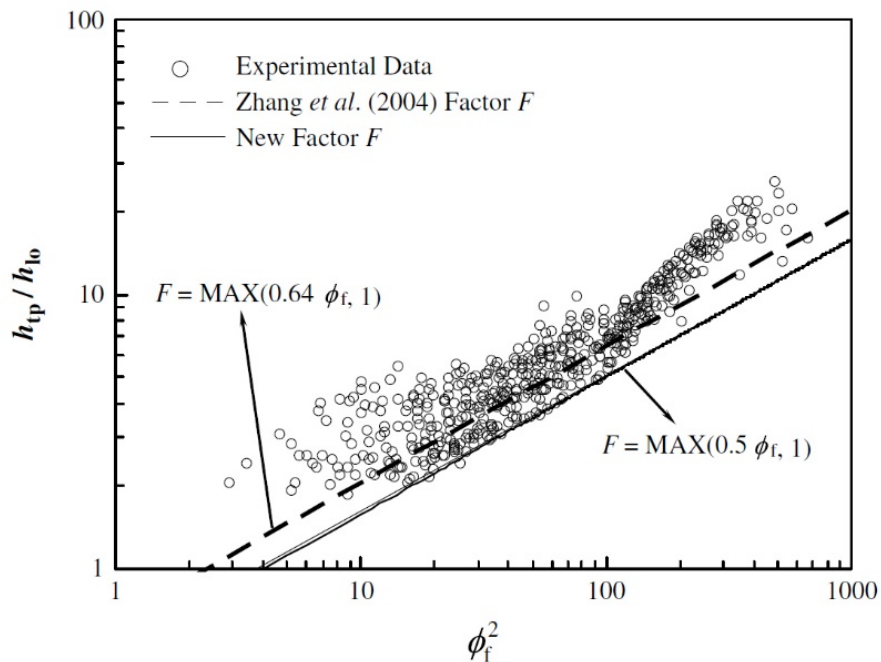


**Figure 12.** Two-phase heat transfer multiplier as a function of $\phi_f^2$
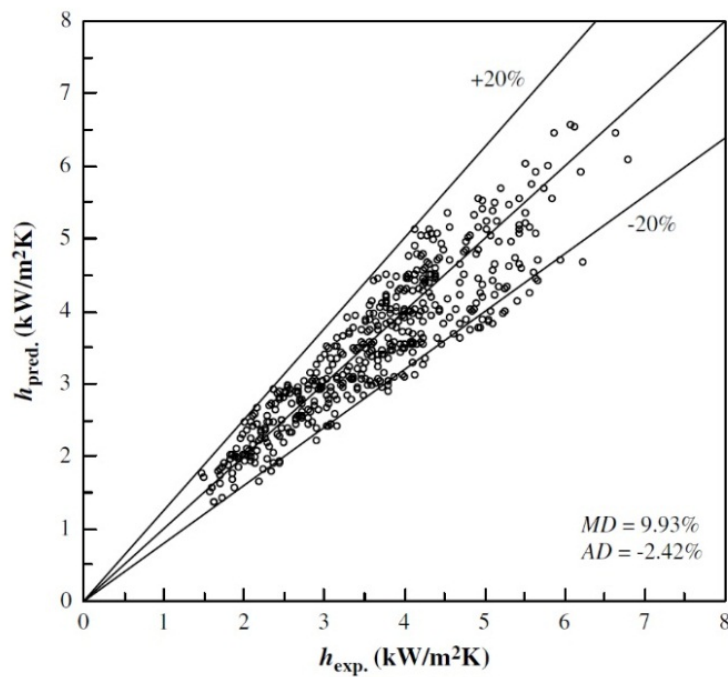
**Figure 13.** Comparison of the experimental and predicted heat transfer coefficients using the new developed correlation

# 5. Concluding remarks

This chapter demonstrated the convective boiling pressure drop and heat transfer experiments of propane in horizontal minichannels. The content is summarized as follows:

1.  The experimental pressure drop of propane was well predicted by the models proposed by Mishima and Hibiki [19], Friedel [20] and Chang et al. [21]

2.  The pressure drop increases with the increase of mass and heat fluxes, and the decrease in the inner tube diameter and saturation temperature. The experimental results illustrated that pressure drop is a function of the mass flux, the tube diameter, the surface tension, the density, and the viscosity.

3.  A new pressure drop correlation was developed on the basis of the Lockhart–Martinelli model. The correlation was defined as a function of the two-phase Reynolds number, $Re_{tp}$, and the two-phase Weber number, $We_{tp}$. In addition, a new factor C was developed using a regression method with a mean and average deviation of 10.84% and 1.08%, respectively.

4.  The effects of mass flux, heat flux, inner tube diameter, and saturation temperature on the heat transfer coefficient of propane were observed. The heat transfer coefficient increases with the decrease in the inner tube diameter and the increase in saturation temperature.

5.    The heat transfer coefficient correlations proposed by Shah [37] and Tran et al. [35] show an accurate prediction with the current heat transfer coefficient experimental data.

6.    The geometric effect of the small tube and flow condition must be considered to develop a new heat transfer coefficient correlation. The development of the enhanced factor F for the convective boiling contribution, and the suppression of factor S for nucleate boiling suppression factor have been also clearly evaluated with the consideration of laminar and turbulent flows. A new boiling heat transfer coefficient correlation that is based on a superposition model for propane in minichannels was demonstrated with 9.93% mean deviation and -2.42% average deviation.

## Nomenclature

$A$: Area (m$^2$)

$AD$: Average deviation, $\mathrm{AD} = \left(\dfrac{1}{n}\right) \sum\limits_1^n \left((\mathrm{d}p_{\mathrm{pred}} - \mathrm{d}p_{\mathrm{exp}}) \times 100 / \mathrm{d}p_{\mathrm{exp}}\right)$

$Bo$: Boiling number, $\mathrm{Bo} = \dfrac{q}{Gi_{\mathrm{fg}}}$

$C$: Chisholm parameter

$c_p$ : Specific heat (kJ kg$^{-1}$ K$^{-1}$)

$D$: Diameter (m)

$f$: Friction factor

$G$: Mass flux (kg m$^{-2}$ s$^{-1}$)

$g$: Acceleration due to gravity (m s$^{-2}$)

$h$: Heat transfer coefficient (kW m$^{-2}$K$^{-1}$)

$i$: Enthalpy (kJ kg$^{-1}$)

$L$: Tube Length (m)

$MD$: Mean deviation, $\mathrm{MD} = \left(\dfrac{1}{n}\right) \sum\limits_1^n \left| \left((\mathrm{d}p_{\mathrm{pred}} - \mathrm{d}p_{\mathrm{exp}}) \times 100 / \mathrm{d}p_{\mathrm{exp}}\right) \right|$

$M$: Molecular weight (kg kmol$^{-1}$)

$n$: Number of data

$p$: Pressure (kPa)

$Q$: Electric power (kW)

$q$: Heat flux (kW m$^{-2}$)

Re: Reynolds number, $Re = \dfrac{GD}{\mu}$

$T$: Temperature (K)

$\dot{m}$: Mass flow rate (kg s$^{-1}$)

$X$: Lockhart-Martinelli parameter

$x$: Vapor quality

$z$: Length (m)

**Greek letters**

$\alpha$: Void fraction

$\Delta i$: The enthalpy rise across the tube (kJ kg$^{-1}$)

$\mu$: Dynamic viscosity (N s m$^{-2}$)

$\rho$: Density (kg m$^{-3}$)

$\sigma$: Surface tension (N m$^{-1}$)

$\phi^2$: Two-phase frictional multiplier

$\Delta T$: Wall super heat (K)

**Gradients and differences**

$(dp/dz)$: Pressure gradient (N m$^{-2}$ m$^{-1}$)

$(dp/dz\ F)$ : Pressure gradient due to friction (N m$^{-2}$m$^{-1}$)

**Subscripts**

crit : Critical point

exp: Experimental value

f: Saturated liquid

fi: Inlet liquid

g: Saturated vapor

i: Inner tube

lo: Liquid only

o: Outlet tube

pb: Pool boiling

pred: Prediction value

r: Reduced

sat: Saturation

sc: Subcooled

t: Turbulent

tp: Two-phase

v: Laminar

w: Wall

wi: Inside tube wall

## Acknowledgements

## Author details

Jong-Taek Oh[1*], Kwang-Il Choi[1] and Nguyen-Ba Chien[2]

*Address all correspondence to: ohjt@chonnam.ac.kr

1 The Department of Refrigeration and Air Conditioning Engineering, Chonnam National University 50 Daehak-ro, Yeosu, Chonnam, Republic of Korea

2 Graduate school, Chonnam National University, 50 Daehak-ro, Yeosu, Chonnam, Republic of Korea

## References

[1] Calm, J. (2008). The next generation of refrigerants – Historical review, considerations, and outlook. International Journal of Refrigeration, 31 (7), 1123–1133.

[2] Palm, B. (2007). Refrigeration systems with minimum charge of refrigerant. Applied Thermal Engineering, 27(10), 1693–1701.

[3] S.S. Bertsch, E.A. Groll, S.V. Garimella, Review and comparative analysis of studies on saturated flow boiling in small channels, Nanoscale Microscale Thermophys. Eng. 12 (3) (2008) 187–227.

[4] V. Dupont, J.R. Thome, Evaporation in microchannels: influence of the channel diameter on heat transfer, Microfluid Nanofluid 1 (2005) 119–127.

[5] Blanco Castro, J., Urchueguía, J., Corberán, J. M., & Gonzálvez, J. (2005). Optimized design of a heat exchanger for an air-to-water reversible heat pump working with propane (R290) as refrigerant: Modelling analysis and experimental observations. Applied Thermal Engineering, 25(14-15), 2450–2462.

[6] Choi, K.-I., Pamitran, a. S., Oh, J.-T., & Saito, K. (2009). Pressure drop and heat transfer during two-phase flow vaporization of propane in horizontal smooth minichannels. International Journal of Refrigeration, 32(5), 837–845. doi:10.1016/j.ijrefrig.2008.12.005

[7] Fernando, P., Palm, B., Ameel, T., Lundqvist, P., & Granryd, E. (2008). A minichannel aluminium tube heat exchanger – Part II: Evaporator performance with propane. International Journal of Refrigeration, 31(4), 681–695. doi:10.1016/j.ijrefrig.2008.02.012

[8] Fernando, P., Palm, B., Lundqvist, P., & Granryd, E. (2004). Propane heat pump with low refrigerant charge: design and laboratory tests. International Journal of Refrigeration, 27(7), 761–773.

[9] Mastrullo, R., Mauro, A.W., Menna, L., & Vanoli, G.P. (2014). Replacement of R404A with propane in a light commercial vertical freezer: A parametric study of performances for different system architectures. Energy Conversion and Management, 82, 54–60. doi:10.1016/j.enconman.2014.02.069

[10] Steiner, D., 1993. VDI-Warmeatlas (VDI Heat Atlas) chapter Hbb. In: Verein Deutscher Ingenieure, editor. VDI- €Gesellschaft Verfahrenstechnik und Chemieingenieurwesen (GCF), Translator: J.W. Fullarton, Dusseldorf.

[11] Premoli, A., Francesco, D., Prina, A., 1971. A dimensionless correlation for determining the density of two-phase mixtures. Lo Termotecnica 25, 17–26.

[12] Chisholm, D., 1972. An equation for velocity ratio in two-phase flow. NEL Report, 535.

[13] Zhao, Y., Molki, M., Ohadi, M. M., Dessiatoun, S.V., 2000. Flow boiling of CO2 in microchannels. ASHRAE Trans, 437–445. DA-00-2-1.

[14] Yoon, S.H., Cho, E.S., Hwang, Y.W., Kim, M.S., Min, K., Kim, Y., 2004. Characteristics of evaporative heat transfer and pressure drop of carbon dioxide and correlation development. Int. J. Refrigeration 27, 111–119.

[15] Park, C.Y., Hrnjak, P.S., 2007. CO2 and R410A flow boiling heat transfer, pressure drop, and flow pattern at low temperatures in a horizontal smooth tube. Int. J. Refrigeration 30, 166–178.

[16] Oh, H.K., Ku, H.G., Roh, G.S., Son, C.H., Park, S.J., 2008. Flow boiling heat transfer characteristics of carbon dioxide in a horizontal tube. Appl. Therm. Eng. 28, 1022–1030.

[17] Cho, J.M., Kim, M.S., 2007. Experimental studies on the evaporative heat transfer and pressure drop of CO2 in smooth and micro-fin tubes of the diameters of 5 and 9.52 mm. Int. J. Refrigeration 30, 986–994.

[18] Chisholm, D., 1967. A theoretical basis for the Lockhart–Martinelli correlation for two-phase flow. Int. J. Heat Mass Transfer 10, 1767–1778.

[19] Mishima, K., Hibiki, T., 1996. Some characteristics of air–water two-phase flow in small diameter vertical tubes. Int. J. Multiphase Flow 22, 703–712.

[20] Friedel, L. Improved friction pressure drop correlations for horizontal and vertical two-phase pipe flow. In: the European Two-phase Flow Group Meeting, Paper E2, June 1979, Ispra, Italy.

[21] Chang, Y.J., Chiang, S.K., Chung, T.W., Wang, C.C., 2000. Two-phase frictional characteristics of R-410A and air-water in a 5 mm smooth tube. ASHRAE Trans, 792–797. DA-00-11-3.

[22] Cicchitti, A., Lombardi, C., Silvestri, M., Solddaini, G., Zavalluilli, R., 1960. Two-phase cooling experiments pressure drop, heat transfer, and burn out measurement. Energia Nucl. 7 (6), 407–425.

[23] McAdams, W.H., 1954. Heat Transmission, third ed. McGraw-Hill, New York.

[24] Beattie, D.R.H., Whalley, P.B., 1982. A simple two-phase flow frictional pressure drop calculation method. Int. J. Multiphase Flow 8, 83–87.

[25] Dukler, A.E., Wicks III, M., Cleveland, R.G., 1964. Frictional pressure drop in two-phase flow: B. An approach through similarity analysis. AIChE J. 10 (1), 44–51.

[26] Lockhart, R.W., Martinelli, R.C., 1949. Proposed correlation of data for isothermal two-phase, two-component flow in pipes. Chem. Eng. Prog. 45, 39–48.

[27] Chisholm, D., 1983. Two-Phase Flow in Pipelines and Heat Exchangers. Longman, New York.

[28] Zhang, M., Webb, R.L., 2001. Correlation of two-phase friction for refrigerants in small-diameter tubes. Exp. Therm. Fluid Sci. 25, 131–139.

[29] Chen, I.Y., Yang, K.S., Chang, Y.J., Wang, C.C., 2001. Two-phase pressure drop of air–water and R-410A in small horizontal tubes. Int. J. Multiphase Flow 27, 1293–1299.

[30] Kawahara, A., Chung, P.M.Y., Kawaji, M., 2002. Investigation of two-phase flow pattern, void fraction and pressure drop in a minichannel. Int. J. Multiphase Flow 28, 1411–1435.

[31] Tran, T.N., Chyu, M.C., Wambsganss, M.W., France, D.M., 2000. Two-phase pressure drop of refrigerants during flow boiling in small channels: an experimental investigation and correlation development. Int. J. Multiphase Flow 26, 1739–1754.

[32] Kew, P.A., Cornwell, K., 1997. Correlations for the prediction of boiling heat transfer in small-diameter channels. Appl. Therm. Eng. 17 (8–10), 705–715.

[33] Lazarek, G.M., Black, S.H., 1982. Evaporative heat transfer, pressure drop and critical heat flux in a small diameter vertical tube with R-113. Int. J. Heat Mass Transfer 25, 945–960.

[34] Wambsganss, M.W., France, D.M., Jendrzejczyk, J.A., Tran, T.N., 1993. Boiling heat transfer in a horizontal small-diameter tube. J. Heat Transfer 115, 963–975.

[35] Tran, T.N., Wambsganss, M.W., France, D.M., 1996. Small circular- and rectangular-channel boiling with two refrigerants. Int. J. Multiphase Flow 22 (3), 485–498.

[36] Bao, Z.Y., Fletcher, D.F., Haynes, B.S., 2000. Flow boiling heat transfer of freon R11 and HCFC123 in narrow passages. Int. J. Heat Mass Transfer 43, 3347–3358.

[37] Shah, M.M., 1978. Chart correlation for saturated boiling heat transfer: equations and further study. ASHRAE Trans 2673, 185–196.

[38] Jung, D.S., McLinden, M., Radermacher, R., Didion, D., 1989. A study of flow boiling heat transfer with refrigerant mixtures. Int. J. Heat Mass Transfer 32 (9), 1751–1764.

[39] Gungor, K.E., Winterton, H.S., 1987. Simplified general correlation for saturated flow boiling and comparisons of correlations with data. Chem. Eng. Res. 65, 148–156.

[40] Takamatsu, H., Momoki, S., Fujii, T., 1993. A correlation for forced convective boiling heat transfer of a non azeotropic refrigerant mixture of HCFC22/CFC114 in a horizontal smooth tube. Int. J. Heat Mass Transfer 36 (14), 3555–3563.

[41] Kandlikar, S.G., Steinke, M.E., 2003. Predicting heat transfer during flow boiling in minichannels and microchannels. ASHRAE Trans, 667–676. CH-03-13-1.

[42] Wattelet, J.P., Chato, J.C., Souza, A.L., Christoffersen, B.R., 1994. Evaporative characteristics of R-12, R-134a, and a mixture at low mass fluxes. ASHRAE Trans, 603–615. 94-2-1.

[43] Chen, J.C., 1966. A correlation for boiling heat transfer to saturated fluids in convective flow. Ind. Eng. Chem. Process Des. Dev. 5, 322–329.

[44] Zhang, W., Hibiki, T., Mishima, K., 2004. Correlation for flow boiling heat transfer in mini-channels. Int. J. Heat Mass Transfer 47, 5749–5763.

[45] Cooper, M.G., 1984. Heat flow rates in saturated nucleate pool boiling–a wide-ranging examination using reduced properties. In: Advances in Heat Transfer, vol. 16. Academic Press, pp. 157–239.

[46] Jung, D., Kim, Y., Ko, Y., Song, K., 2003. Nucleate boiling heat transfer coefficients of pure halogenated refrigerants. Int. J. Refrigeration 26, 240–248.